Journal for ImmunoTherapy of Cancer

Impact of CD4 T cells on intratumoral CD8 T-cell exhaustion and responsiveness to PD-1 blockade therapy in mouse brain tumors

Saad M Khan,[1] Rupen Desai ,[1] Andrew Coxon,[1] Alexandra Livingstone,[2] Gavin P Dunn ,[3] Allegra Petti,[1] Tanner M Johanns[2]

To cite: Khan SM, Desai R, Coxon A, *et al*. Impact of CD4 T cells on intratumoral CD8 T-cell exhaustion and responsiveness to PD-1 blockade therapy in mouse brain tumors. *Journal for ImmunoTherapy of Cancer* 2022;**10**:e005293. doi:10.1136/jitc-2022-005293

► Additional supplemental material is published online only. To view, please visit the journal online (http://dx.doi.org/10.1136/jitc-2022-005293).

SMK and RD contributed equally.

Accepted 28 November 2022

[1]Department of Neurosurgery, Washington University in St Louis School of Medicine, St Louis, Missouri, USA
[2]Department of Medicine, Division of Medical Oncology, Washington University in St Louis School of Medicine, St Louis, Missouri, USA
[3]Department of Neurosurgery, Massachusetts General Hospital, Boston, Massachusetts, USA

Correspondence to
Dr Tanner M Johanns;
tjohanns@wustl.edu

ABSTRACT

Background Glioblastoma is a fatal disease despite aggressive multimodal therapy. PD-1 blockade, a therapy that reinvigorates hypofunctional exhausted CD8 T cells (T_{ex}) in many malignancies, has not shown efficacy in glioblastoma. Loss of CD4 T cells can lead to an exhausted CD8 T-cell phenotype, and terminally exhausted CD8 T cells (T_{ex}^{term}) do not respond to PD-1 blockade. GL261 and CT2A are complementary orthotopic models of glioblastoma. GL261 has a functional CD4 T-cell compartment and is responsive to PD-1 blockade; notably, CD4 depletion abrogates this survival benefit. CT2A is composed of dysfunctional CD4 T cells and is PD-1 blockade unresponsive. We leverage these models to understand the impact of CD4 T cells on CD8 T-cell exhaustion and PD-1 blockade sensitivity in glioblastoma.

Methods Single-cell RNA sequencing was performed on flow sorted tumor-infiltrating lymphocytes from female C57/BL6 mice implanted with each model, with and without PD-1 blockade therapy. $CD8^+$ and $CD4^+$ T cells were identified and separately analyzed. Survival analyses were performed comparing PD-1 blockade therapy, CD40 agonist or combinatorial therapy.

Results The CD8 T-cell compartment of the models is composed of heterogenous CD8 T_{ex} subsets, including progenitor exhausted CD8 T cells (T_{ex}^{prog}), intermediate T_{ex}, proliferating T_{ex}, and T_{ex}^{term}. GL261 is enriched with the PD-1 responsive T_{ex}^{prog} subset relative to the CT2A and CD4-depleted GL261 models, which are composed predominantly of the PD-1 blockade refractory T_{ex}^{term} subset. Analysis of the CD4 T-cell compartments revealed that the CT2A microenvironment is enriched with a suppressive T_{reg} subset and an effector CD4 T-cell subset that expresses an inhibitory interferon-stimulated (*Isc*) signature. Finally, we demonstrate that addition of CD40 agonist to PD-1 blockade therapy improves survival in CT2A tumor-bearing mice.

Conclusions Here, we describe that dysfunctional CD4 T cells are associated with terminal CD8 T-cell exhaustion, suggesting CD4 T cells impact PD-1 blockade efficacy by controlling the severity of exhaustion. Given that CD4 lymphopenia is frequently observed in patients with glioblastoma, this may represent a basis for resistance to PD-1 blockade. We demonstrate that CD40 agonism may circumvent a dysfunctional CD4 compartment to improve PD-1 blockade responsiveness, supporting a novel synergistic immunotherapeutic approach.

WHAT IS ALREADY KNOWN ON THIS TOPIC

⇒ CD4 T cells promote a functional CD8 T-cell response, while CD4 T-cell deficiency drives increased CD8 T-cell exhaustion in settings of chronic antigen stimulation, like cancer. CD4 T cells are required for PD-1 blockade efficacy, while terminally exhausted CD8 T cells (T_{ex}^{term}) are unresponsive to PD-1 blockade. Glioblastoma is a demonstrably CD4-deficient tumor and unresponsive to PD-1 blockade therapy. The underlying basis for the resistance to PD-1 blockade in glioblastoma is unknown.

WHAT THIS STUDY ADDS

⇒ Our results demonstrate that efficacy of PD-1 blockade therapy in brain tumors is reliant on a responsive subset of CD8 T cells maintained by functional CD4 T cells; however, a dysfunctional CD4 T-cell compartment may be circumvented with synergistic pharmacotherapies.

HOW THIS STUDY MIGHT AFFECT RESEARCH, PRACTICE OR POLICY

⇒ The findings here suggest that future immunotherapy for glioblastoma will augment or circumvent the CD4 T-cell compartment to optimize the reactivation of exhausted CD8 T cells.

INTRODUCTION

The implementation of checkpoint blockade therapy, an immunotherapy centered on reinvigorating an exhausted immunological response, has fundamentally altered oncology. However, clinical benefit has not yet been observed in glioblastoma.[1] Although once considered an 'immunologically privileged' microenvironment, mounting data demonstrate active immune monitoring within the central nervous system (CNS), particularly in the diseased state with associated disruption of the blood–brain barrier.[2] The presence of

CNS immunosurveillance is underscored by the fact that metastatic disease to the brain responds to checkpoint therapy equivalently to extracranial disease.[3] Therefore, the lack of response to checkpoint blockade therapy in glioblastoma is likely a disease-specific rather than a site-specific phenomenon, underscoring the need to better understand glioblastoma immunobiology.

PD-1 blockade relinquishes inhibitory signals and upregulates effector function of exhausted tumor-specific T cells, leading to restoration of antitumor immunity. Exhausted CD8 T cells (T_{ex}) are a distinct T-cell lineage defined by the progressive loss of proliferative capacity and secretory effector cytokine production.[4 5] T_{ex} subsets were initially defined in mouse chronic viral infection models, in which dysfunction was correlated with progressive expression of inhibitory cell surface proteins such as PD-1, LAG3, and TIM-3.[6] The application of single-cell technologies has provided additional granularity to the extensive heterogeneity of this lineage. Importantly, T_{ex} subsets with differential responsiveness to checkpoint blockade have been characterized: PD-1 blockade-responsive progenitor exhausted CD8 T cells (T_{ex}^{prog}) and unresponsive terminally exhausted CD8 T cells (T_{ex}^{term}).[4 6–11] The T_{ex}^{prog} population is defined by retained *Tcf7* expression, critical to both maintain self-renewal and reactivate effector cytokine production.[8] Conversely, in the T_{ex}^{term} subset, *Tcf7* expression is lost, driving reduced proliferative potential, downregulated effector cytokines, and increased expression of coinhibitory immune checkpoint molecules through the high-mobility group box DNA-binding transcription factor, TOX. The progressive development of this T_{ex}^{term} state is driven by chronic antigen stimulation. Thus, one potential mechanism for glioblastoma resistance to PD-1 blockade therapy is a predominance of unresponsive T_{ex}^{term}.[6 9 12]

To evaluate this hypothesis, we studied two complementary murine glioblastoma models, GL261 and CT2A, with differential responsiveness to PD-1 blockade. While PD-1 blockade improves survival in mice with established intracranial GL261 tumors, PD-1 blockade is completely ineffective in mice bearing CT2A tumors.[13 14] Despite the differences in sensitivity to PD-1 blockade therapy, these models share key similarities: (1) carcinogen induction with high mutational loads, (2) progressive growth when orthotopically transplanted into syngeneic C57BL/6 mice, and (3) well-defined Major Histocompatibility Complex (MHC) class I-restricted neoantigens that endogenously prime neoantigen-specific CD8 T cells. Thus, comparative analysis of these two models may provide insights into the underlying basis for lack of PD-1 blockade efficacy in brain tumors.

Prior studies have shown CD4 T-cell deficiency in both murine chronic viral infection models and HIV-positive patients leads to increased expression of exhaustion markers on CD8 T cells, suggesting CD4 T cells restrict the development of a more severe CD8 T-cell exhaustion phenotype.[5 15] We have previously shown that there are significantly fewer CD4 T cells infiltrating CT2A tumors compared with GL261 tumors, and the CT2A-infiltrating CD4 T cells that are present are more dysfunctional than GL261-derived CD4 tumor-infiltrating lymphocytes (TILs).[14 16] Similarly, when CD4 T cells are pharmacologically depleted from GL261 tumor-bearing mice, PD-1 blockade is ineffective.[17] These observations suggest CT2A-depleted and CD4-depleted GL261 serve as useful models to evaluate the importance of CD4 T cells on CD8 T-cell exhaustion, which has direct relevance to the CD4-deficient state observed in patients with glioblastoma.

We used single-cell RNA sequencing (scRNA-seq) to analyze the tumor-infiltrating T cells of these three tumor models and observed a gradient of T_{ex} that closely resembles previously described T_{ex}^{term} and T_{ex}^{prog} subsets. Furthermore, we demonstrate that the PD-1 blockade-responsive GL261 model is enriched for T_{ex}^{prog} cells, while the PD-1 blockade-unresponsive CT2A model is predominantly composed of T_{ex}^{term} cells. Consistent with the previously described role of CD4 T-cell loss in driving more severe CD8 T-cell exhaustion in mouse models and human disease, we note that CD4 T-cell depletion is associated with an abrogated survival benefit to PD-1 blockade and leads to development of a T_{ex}^{term} predominant CD8 T-cell population in GL261 that closely mirrors that of CT2A. Finally, we find administration of a CD40 agonist to circumvent CD4 T-cell deficiency is therapeutically synergistic when combined with PD-1 blockade in the CD4 T cell-dysfunctional CT2A model but not in the CD4 T cell-proficient GL261 model.

METHODS

Animals and tumor implantation

C57BL/6 female mice (Jackson Laboratory) 8–10 weeks old were acclimated for 2 weeks in specific pathogen-free housing. GL261 was obtained from the National Cancer Institute Tumor Repository, CT2A was obtained from Dr Peter Fecci (Duke University). Tumor cells (5×10^4) were resuspended in 5 µL phosphate-buffered saline and stereotactically injected into the right striatum of anesthetized mice and randomly distributed into cages representing experimental group, providing age-matched and litter-matched cohorts. Given the nature of subsequent treatments and analyses, the cohorts were not blinded.

Checkpoint inhibitor, CD4 depleting antibody, and CD40 agonist dosing

Anti-PDL1 antibody, anti-CD4 depletion antibody, and anti-CD40 agonist were purchased from BioXCell. For scRNA-seq experiments, when indicated, 200 mg CD4 depleting antibody was administered intraperitoneally on day 5 after tumor implantation, and 200 mg of anti-PDL1 was administered intraperitoneally on day 11 after tumor implantation. TIL were harvested on day 14 post implantation. For survival experiments, anti-PDL1 and CD40 agonist were dosed as follows: GL261—CD40 agonist on day 9, anti-PDL1 on days 11, 15, and 19; and CT2A—CD40 agonist on day 7, anti-PDL1 on days 9, 12, 16, and 21 for

CT2A. CD4 depletion antibody was administered on day 5 and weekly thereafter. Mortality was recorded or mice were euthanized on reaching predetermined humane endpoints after daily monitoring for neurological deficits, signs of suffering, or impaired function. Kaplan-Meier survival analyses were conducted in GraphPad Prism using Mantel-Cox test. All mice were included for scRNA-seq and survival analyses.

TIL harvesting and T-cell flow cytometric enrichment/analysis

For scRNA-seq experiments, mice were euthanized on postimplantation day 14 (pooled n=3 per model to ensure sufficient cells). Tumors were harvested, dissociated, and filtered through a 70 micron cell strainer. Red blood cells were removed with ACK lysis solution (Thermo Fischer Scientific), and a Percoll density gradient (Sigma-Aldrich) was used for myelin removal. Cell surface staining was performed for live cells (Zombie NIR, BioLegend), CD3 (BioLegend), and CD11b (BioLegend), and cells were sorted on a BD FACSARIAII flow sorter, enriching the live $CD3^+CD11b^-$ cell population to represent 75% of the total population for further analyses. For intracellular cytokine/transcription factor staining, tumor infiltrating lymphocytes were isolated as previously mentioned then stained using the True-Nuclear Transcription Factor Buffer Kit (BioLegend) with CD45 AlexaFluor700, CD3 PerCP/Cy5.5, CD4 PE/Cy7, CD8 PE Dazzle564, Zombie NIR, PD-1 BV650, Foxp3 BV421 (BioLegend); TCF1 AlexaFluor488 (BD Biosciences); and TOX PE and IL-21 APC (eBiosciences) per manufacturer's instructions. Quantification of interleukin (IL)-21 was performed by gating on live (Zombie NIR negative) $CD3^+CD8^-CD4^+Foxp3^-$ cells. For quantification of TOX and TCF1, gating was on live $CD3^+CD8^+CD4^-PD\text{-}1^+$ cells. The absolute number of TIL was determined by performing a cell count on isolated cells using a hemocytometer and then calculating the number of immune subsets based on flow cytometry analysis (ie, for $CD8^+$ TIL=number of cells per sample×%$CD45^+$×%$CD3^+CD8^+$). Analysis was performed on FlowJo software V.10.6.0 and statistical analysis was performed on Prism GraphPad.

scRNA-seq library generation

A live single-cell suspension of $CD3^+CD11b^-$ cells were resuspended at 1000 cells/µL in phosphate-buffered saline with 0.04% bovine serum albumin. Single-cell RNA libraries were generated using the Chromium Next GEM Single Cell 5' library and Gel Bead Kit v1.1; T Cell Receptor (TCR) enrichment was performed with the Chromium Single Cell V(D)J Enrichment Kit for Mouse T cells as per manufacturer's protocol (10X Genomics). Library quality and concentration were determined using a Bioanalyzer Tapestation (Agilent) for library sequencing on the NovaSeq 6000 instrument at a sequencing depth of ~50K read pairs per cell.

scRNA-seq computational analyses

Cell Ranger V.3.0.1 (10X Genomics) was used to process, align, and generate feature-barcode matrices against the mouse reference genome. Transcriptomic data were analyzed with the Seurat R package193- V.3.2.3.[18] scRNA-seq libraries underwent doublet filtering (cells with greater than 93rd percentile with respect to nCount were removed), and cells with <500 features or >5% mitochondrial content were removed prior to log normalization, cell cycle scoring, and scaling. Dimensionality reduction was performed using PCA and Uniform Manifold Approximation and Projection (UMAP), with principal components selected using the ElbowPlot and JackStraw functions. As previously described, unsupervised cell type inference was performed by training a nearest neighbor algorithm on expression data from mouse Haemopedia.[19 20] Cell type predictions were further combined with CD4 and CD8 expression to define whole clusters as either $CD4^+$ and $CD8^+$ T-cell clusters; non-T-cell clusters were not included in subsequent analyses. To address the potential impact of transcript 'drop-out' in cell type identification, subsequent $CD8^+$ analyses were repeated with additional rigorous filtering criteria requiring *CD8* expression of >0, with no change in the results (data not shown). The $CD4^+$ and $CD8^+$ clusters were individually subsetted and again underwent log normalization and scaling prior to dimensionality reduction for further analyses. Thirty principal components at a cluster resolution of 0.7 were used for CD8 analyses, and 20 principal components at a cluster resolution of 0.9 were used for CD4 analyses. Distributions of UMIs per cell per treatment condition and cell cycle were visualized using the ggplot2 R package. Differentially expressed genes between groups in each cluster were detected using a Wilcoxon rank-sum test from the *FindAllMarkers* function in the Seurat R package. The expression of the following genes was used to generate a CD8 T-cell exhaustion score using the Seurat package *AddModuleScore: LAG3*, *CTLA4*, *PDCD1*, *HAVCR2*, *TOX*, *ICOS*, *TNFRSF4*, and *TIGIT*. Functional enrichment was calculated using the clusterProfiler package.[21]

V(D)J libraries were processed with CellRanger V(D)J V.3.0.1 (10X Genomics) mapped onto a mouse V(D)J reference genome. Clonotype analysis was performed with the scRepertoire R package V.1.3.1, using the functions quantContig, clonalHomeostasis, clonalProportion, and clonalDiversity.[22]

RESULTS

scRNA-seq of TIL from established intracranial murine gliomas reveals a gradient of exhausted CD8 T-cell states

To study the T-cell populations in murine gliomas with or without PD-1-blockade therapy, mice were implanted intracranially with GL261 or CT2A and allowed to establish over 11 days, at which time half the mice in each group were treated with anti-PDL1 antibody. TILs were harvested 3 days later, and $CD3^+CD11b^-$ TILs were enriched by flow sorting and submitted for scRNA-seq. The $CD8^+$ population was initially analyzed, and graph-based clustering demonstrated 11 distinct clusters (online supplemental figure S1A). On manual review, clusters 9

and 10 were present exclusively in untreated CT2A and CD4-depleted anti-PDL1 treated GL261, respectively (online supplemental figure S1B). Interestingly, the most highly enriched genes in these clusters were related to the T-cell receptor, suggesting an expanded monoclonal/oligoclonal population may be driving the clustering. Indeed, clonotype analysis demonstrated that these clusters were each composed of monoclonal populations (data not shown). We therefore removed TCR-related genes (online supplemental table 1) and reran scaling, log transformation, and variable gene selection of the CD8 T cells using 31 principal components at a cluster resolution of 0.7. After excluding TCR genes, graph-based clustering of these 5154 cells yielded eight clusters (figure 1A), with redistribution of the expanded oligoclonal cells throughout these clusters (online supplemental figure S1C).

We first sought to identify T_{ex}^{prog} and T_{ex}^{term} subsets using previously established marker genes, which corresponded to distinct cell clusters, several expressing T_{ex}^{term} markers (clusters 0, 3, 4, and 7) and one expressing T_{ex}^{prog} markers (cluster 1) (figure 1B). We generated a composite exhaustion score using T_{ex}^{term} marker genes (see the Methods section) (online supplemental figure S2). This indicated a gradient of exhaustion from cluster 1 (least exhausted) to clusters 0, 3, 4, and 7 (most exhausted) (figure 1C). Consistently, *Tcf7*, a T_{ex}^{prog} marker, was inversely correlated with exhaustion score and predominantly enriched in cluster 1. We then scored each cell for expression of genes associated with the T_{ex}^{term} signature defined in previously published datasets including murine chronic viral and cancer models.[7 12] We again noted that clusters 0, 3, 4, and 7 aligned with the T_{ex}^{term} signature (online supplemental figure S3). To identify the cellular processes unique to the four T_{ex}^{term} clusters, we first identified global differentially expressed genes for each cluster, then analyzed their functional enrichment (online supplemental figure S4). Combined with *Ki67* expression (figure 1D), this revealed upregulation of cell division and proliferative pathways in clusters 3 and 7, suggesting these clusters represent the previously described proliferating T_{ex} cells (T_{ex}^{prolif}), which progressively lose *Tcf7* expression as they divide and convert into an irreversible terminally exhausted state.[8] Collectively, these data suggest that clusters 0 and 4 represent a T_{ex}^{term} transcriptional state; clusters 3 and 7 align with a T_{ex}^{prolif} transcriptional state; and cluster 1 is consistent with a T_{ex}^{prog} transcriptional state. Together, these results demonstrate that $CD8^+$ TIL isolated from these two orthotopic glioblastoma mouse models correspond to previously defined CD8 T cell-exhausted states, and the full differentiation gradient of this distinct T-cell lineage is represented.

GL261 and CT2A TILs consist of progenitor and terminally exhausted populations that differentially respond to PD-1 blockade therapy and are mediated by CD4 T cells

We next assessed the frequency of each T_{ex} subset within $CD8^+$ TIL isolated from GL261 and CT2A tumor-bearing mice. Notably, GL261 was enriched in T_{ex}^{prog}, while CT2A was predominantly composed of T_{ex}^{term} (figure 2). In extracranial tumor models, it has been shown that PD-1 blockade therapy reinvigorates T_{ex}^{prog} but not T_{ex}^{term}.[10] To determine if this holds true in intracranial tumors, we profiled the transcriptional changes induced by PD-1 blockade therapy in GL261 and CT2A. Similar to observations in extracranial tumors,[11 12 23] the T_{ex}^{prog} enriched GL261 $CD8^+$ TIL demonstrated a shift in transcriptional activity following PD-1 blockade therapy from cluster 1 (T_{ex}^{prog} signature) to clusters 2 and 5, while the largely T_{ex}^{term} $CD8^+$ subset of CT2A did not exhibit a substantial transcriptional change (figure 2). To further define the transcriptional changes of $CD8^+$ TIL in GL261 following PD-1 blockade, cluster 5 was analyzed more closely and found to have adopted an early exhausted state with upregulation of several checkpoint molecules (figure 1C). As clusters 2 and 6 demonstrate similar early upregulation of exhaustion markers, these three clusters likely represent an intermediate exhausted CD8 T-cell (T_{ex}^{inter}) state. Moreover, the presence of a T_{ex}^{inter} is consistent with lineage tracking experiments demonstrating that T_{ex}^{prog} CD8 T cells differentiate into T_{ex}^{term} CD8 T cells following checkpoint blockade therapy[10] and confirmed in our data by performing a trajectory analysis which placed cluster 5 transitionally between the T_{ex}^{prog} and T_{ex}^{term} clusters (online supplemental figure S7). Furthermore, cluster five shows increased expression of genes previously shown to be upregulated in PD-1 blockade-responsive CD8 T cells (online supplemental figure S8).[6 9 11]

To further validate these transcriptional findings identified between $CD8^+$ TIL in GL261 and CT2A on a protein level, we quantified expression of the T_{ex}^{prog}-defining transcription factor, TCF1 (encoded by *Tcf7*) by flow cytometry. In GL261, approximately 40% of $CD8^+$ TIL are $TCF1^+$, in contrast to only 10% of $CD8^+$ TIL that are $TCF1^+$ in CT2A (figure 3). Conversely, roughly 90% of $CD8^+$ TILs isolated from CT2A express the T_{ex}^{term}-defining transcription factor, TOX, compared with 55% in GL261 (figure 3B). While both GL261 and CT2A contain TOX^+CD8^+ TIL, the level of TOX expression is significantly lower in GL261 $CD8^+$ TIL than CT2A (figure 3C), though the functional consequence of differences in expression level is unclear. Following PD-1 blockade, there was a significant decrease in TCF1-expressing $CD8^+$ TIL in GL261, similar to what was noted transcriptionally along with a corresponding increase in TOX-expressing $CD8^+$ TIL. In contrast, the percentage of these two populations remained relatively unchanged in CT2A after PD-1 blockade treatment (figure 3A,B), which also paralleled the scRNA-seq data. Thus, the preferential distribution of T_{ex}^{prog} in GL261 and T_{ex}^{term} in CT2A is consistent with the observed differential responsiveness of these two models to PD-1 blockade.

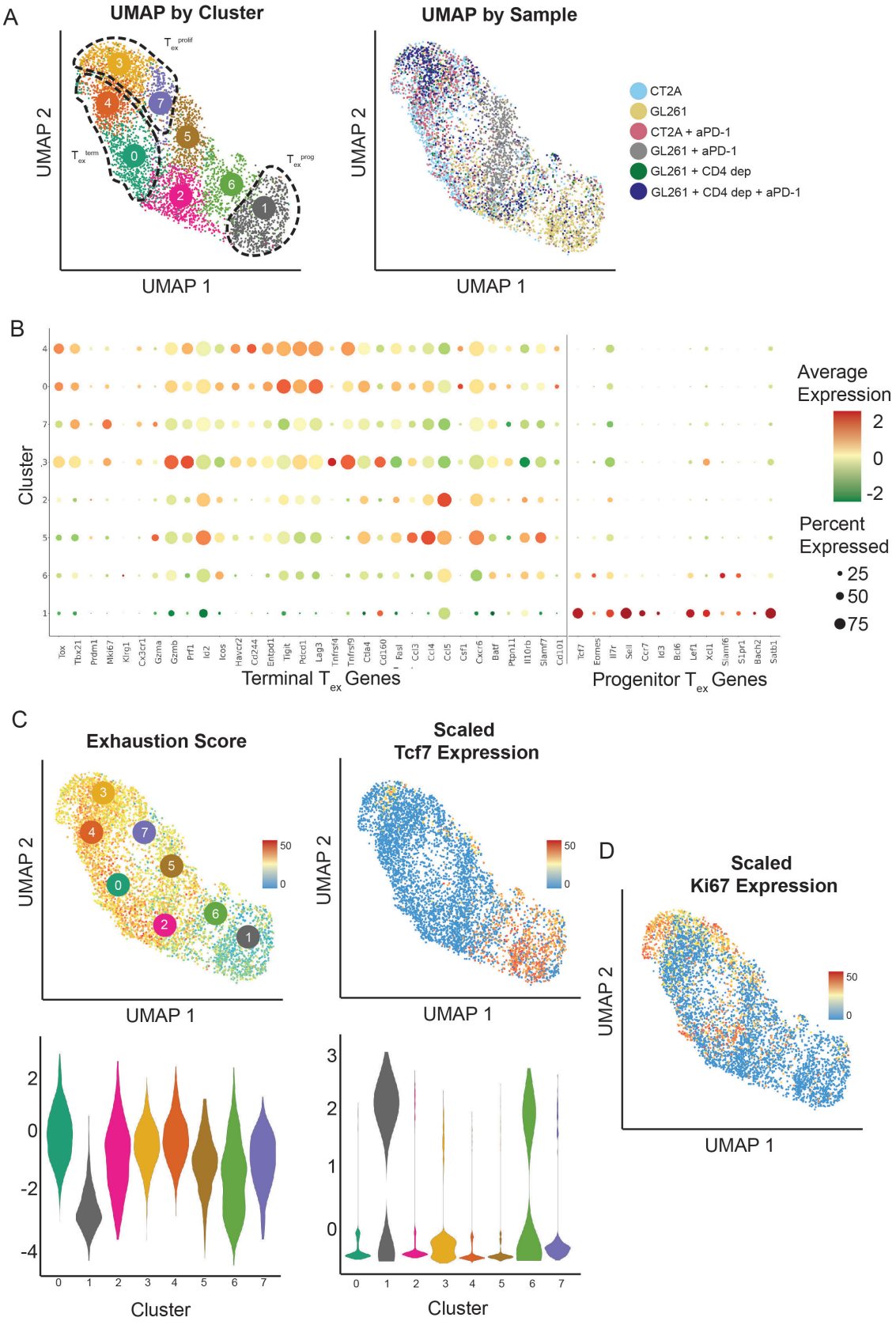

Figure 1 Single-cell RNA-sequencing characterization of infiltrating CD8$^+$ T cells in six glioma models. (A) UMAP with cells colored according to graph-based cluster on the left (T_{ex} subsets defined in subsequent analyses) and by glioma model on the right. (B) Gene expression dot plot of key genes associated with terminal and progenitor exhausted T-cell (T_{ex}) populations, which defines cluster 1 as T_{ex}^{prog}. (C) UMAP and violin plot of left exhaustion module score and right expression of *Tcf7*. (D) UMAP feature plot of *Ki67* expression supports clusters 3 and 7 as a T_{ex}^{prolif} subset. T_{ex}, exhausted CD8 T cell; T_{ex}^{prog}, progenitor exhausted CD8 T cell; T_{ex}^{prolif}, proliferating T_{ex} cell.

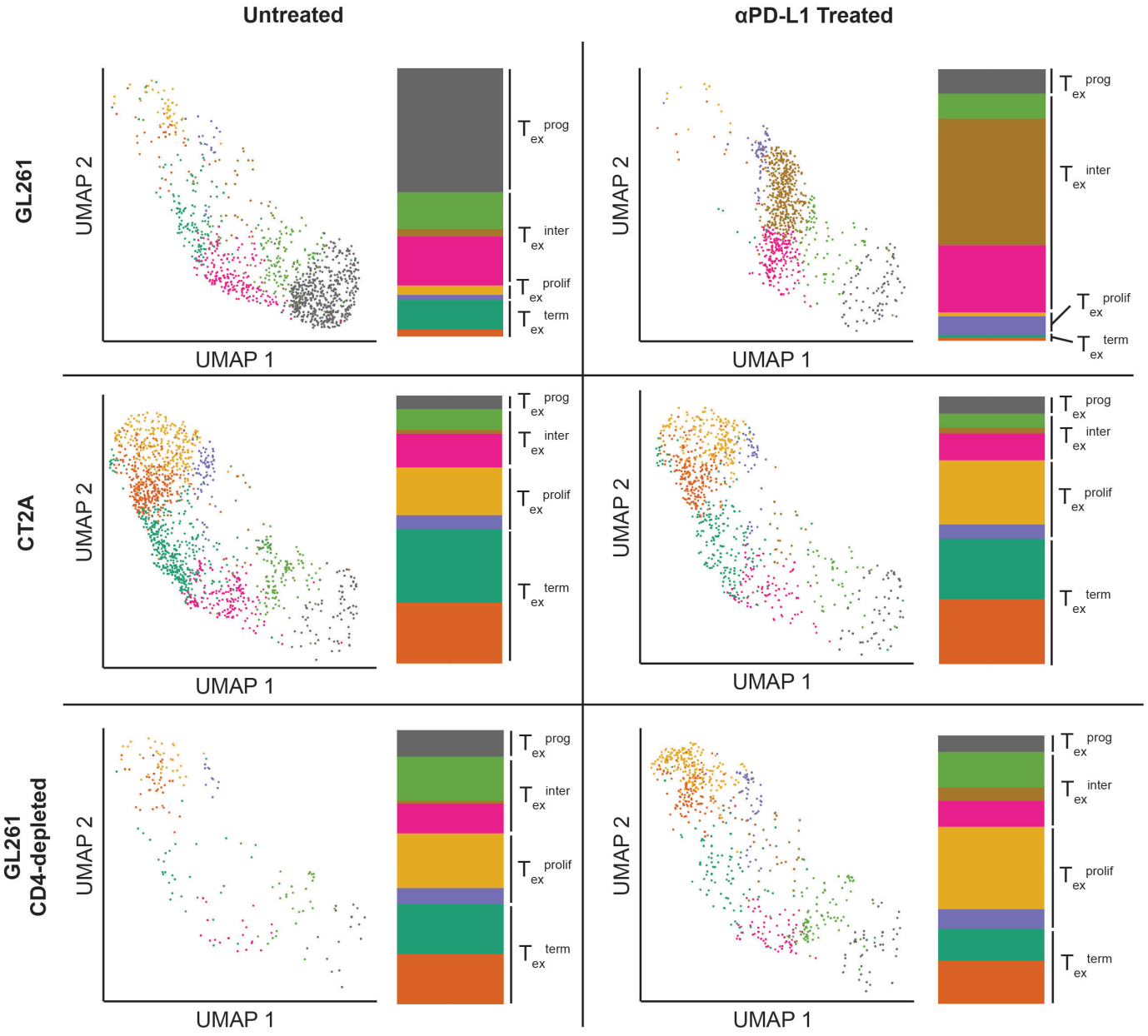

Figure 2 Effect of murine glioma model and PD-1 blockade therapy on CD8$^+$ T-cell compartment. For each model: left UMAP of CD8$^+$ T cells, right histogram of cell composition in each cluster. While GL261 shifts from a T_{ex}^{prog} to T_{ex}^{inter} predominant model following PD-1 blockade therapy, the CD4-deficient models (CT2A and CD4-depleted GL261) are composed of T_{ex}^{term} cells that are not affected by PD-1-blockade therapy. T_{ex}, exhausted CD8 T cell; T_{ex}^{inter}, intermediate exhausted CD8 T cell; T_{ex}^{prog}, progenitor exhausted CD8 T cell; T_{ex}^{prolif}, proliferating T_{ex} cell; T_{ex}^{term}, terminally exhausted CD8 T cell.

One potential alternative explanation for differences in responsiveness to PD-1 blockade therapy between these two models is a lack of immune cell infiltration into the CT2A microenvironment compared with GL261. We therefore quantified total numbers of CD8$^+$ and CD4$^+$ TIL among these two models and, in fact, noted an increased number of CD8$^+$ TIL in CT2A compared with GL261 (online supplemental figure S5A), which is supported by the presence of a higher frequency of T_{ex}^{prolif} in CT2A (figure 2). Thus, these data suggest that differences in PD-1 blockade responsiveness is not simply due to lack of effector CD8 T-cell infiltration into CT2A.

These data also demonstrate CT2A is not a numerically CD4 lymphopenic tumor microenvironment (online supplemental figure S5A). However, we have previously demonstrated that the CD4$^+$ TILs present in CT2A display a more dysfunctional effector profile than CD4$^+$ TILs from GL261,[14] suggesting CT2A may represent a functionally CD4 deplete microenvironment. Given the previously suggested role of CD4 T cells in restraining the development of T_{ex}^{term} CD8 T cells described in chronic Lymphocytic Choriomeningitis virus (LCMV),[8] we tested the hypothesis that the response to PD-1 blockade and transcriptional profile of CD8$^+$ TIL in GL261-bearing

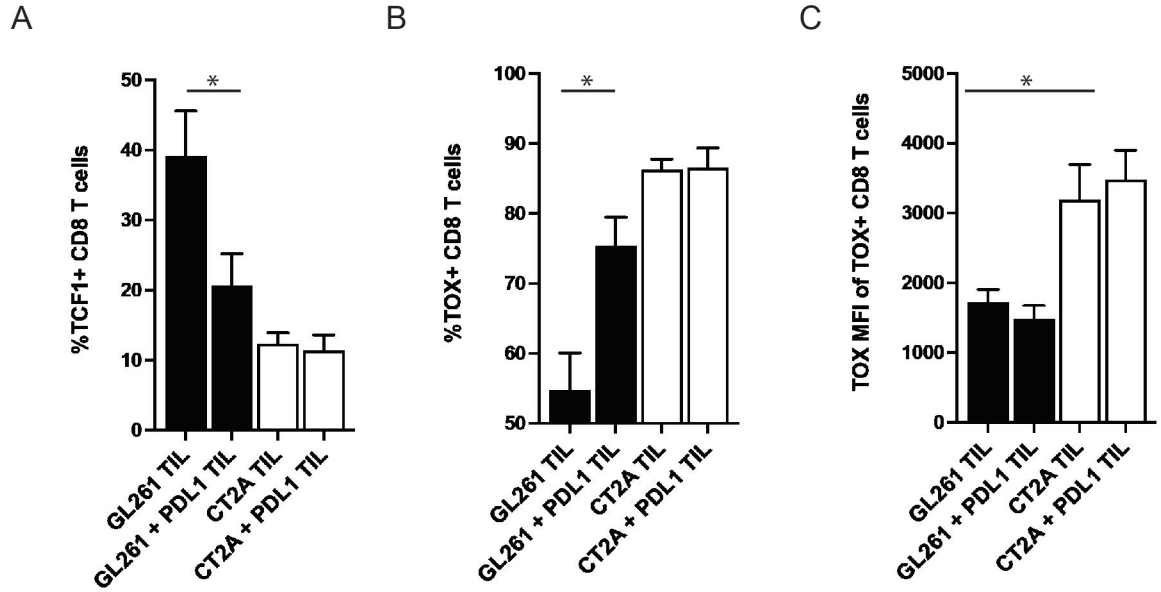

Figure 3 Differences in TCF1 and TOX expression among CD8$^+$ TIL isolated from GL261 and CT2A with and without PD-1 blockade therapy. (A) Bar graph depicting percentage TCF1$^+$PD-1$^+$CD8$^+$ TIL among total PD-1$^+$CD8$^+$ TIL in GL261 and CT2A with and without anti-PDL1 antibody treatment (GL261 TIL vs CT2A TIL, p=0.0025; GL261 TIL vs GL261+PDL1 TIL, p=0.021). (B) Bar graph depicting percentage TOX$^+$PD-1$^+$CD8$^+$ TIL among total PD-1$^+$CD8$^+$ TIL in GL261 and CT2A with and without anti-PDL1 antibody treatment (GL261 TIL vs CT2A TIL, p=0.0003; GL261 TIL vs GL261+PDL1 TIL, p=0.0057). (C) Bar graph representing mean fluorescent intensity of TOX expression in TOX$^+$PD-1$^+$CD8$^+$ TIL (GL261 TIL vs CT2A TIL, p=0.0069). Data pooled from at least two independent experiments with n=3 mice per group per experiment. TIL, tumor-infiltrating lymphocyte.

mice in the setting of CD4 depletion would similarly mirror CT2A. Consistent with this hypothesis, pharmacological depletion of CD4-expressing T cells in GL261 abrogates the survival benefit to PD-1 blockade therapy (online supplemental figure S6) with a corresponding predominance of T_{ex}^{term} CD8$^+$ TIL population unaffected by PD-1 blockade therapy (figure 2). Furthermore, similar to CT2A, CD8$^+$ TIL from CD4-depleted GL261 had an increase in T_{ex}^{prolif} (figure 2) and absolute numbers of CD8$^+$ TIL compared with CD4-intact GL261-bearing mice (online supplemental figure S5B). It should also be noted that the relative paucity of T_{ex}^{prog} in both CD4-deficient brain tumor models (CT2A-depleted and CD4-depleted GL261) is in slight contrast to the chronic viral infection model, LCMV, where CD4 depletion leads to an increase in T_{ex}^{term} via progressive differentiation of a T_{ex}^{inter} population but preservation of the T_{ex}^{prog} population.[24] Thus, there may a context-dependent role of CD4 T cells on T_{ex}^{prog} differentiation influenced by pathology (infection vs tumor) and/or location (intracranial vs extracranial).

In summary, GL261 is composed of T_{ex}^{prog}-predominant CD8$^+$ TIL capable of responding to PD-1 blockade therapy, while CT2A-depleted and CD4-depleted GL261 CD8$^+$ TILs represent a T_{ex}^{term} subset insensitive to PD-1 blockade therapy. Together, these findings support the potential role of CD4 T cells to mediate PD-1 blockade therapy efficacy by restricting CD8 T cells from differentiating into an unresponsive T_{ex}^{term} state.

CT2A TIL consists of highly expanded TCR clonotypes, while GL261 has preserved TCR diversity

The emergence of clonally expanded, terminally differentiated CD8 T cells in response to persistent antigen exposure has been described in models of chronic viral infection.[7] We therefore analyzed T-cell clonality in these tumor models using the Shannon and Simpson Indices, measures of TCR diversity, which demonstrated GL261 had a more diverse clonotypic repertoire than CT2A (online supplemental figure S9). We ranked clonotypes based on their frequency, assigning a clonal index to each TCR with the dominant clonotype represented by a clonal index of 1 (figure 4). In both tumor models, clonal expansion is higher in the T_{ex}^{term} clusters. This finding is replicated by superimposing clonal groups (defined by degree of expansion) onto the CD8 T-cell UMAP (figure 4B) or the top five clonal indices split by sample (figure 4C). Given the effects of CD4 depletion on the composition of the GL261 CD8$^+$ TIL compartment, we evaluated its effects on TCR heterogeneity and found CD4 depletion in GL261 similarly reduces the clonal diversity near that of CT2A (figure 4A,C).

As proliferation of exhausted *Tcf7*-expressing progenitor CD8 T cells in response to checkpoint blockade therapy has been described in chronic viral models, we next assessed the influence of PD-1 blockade therapy on the CD8 T-cell compartment in each tumor model.[6] As anticipated, given the relative enrichment of T_{ex}^{prog} in GL261, we observed clonal expansion in GL261 CD8$^+$ TIL following PD-1 blockade therapy with an accompanying

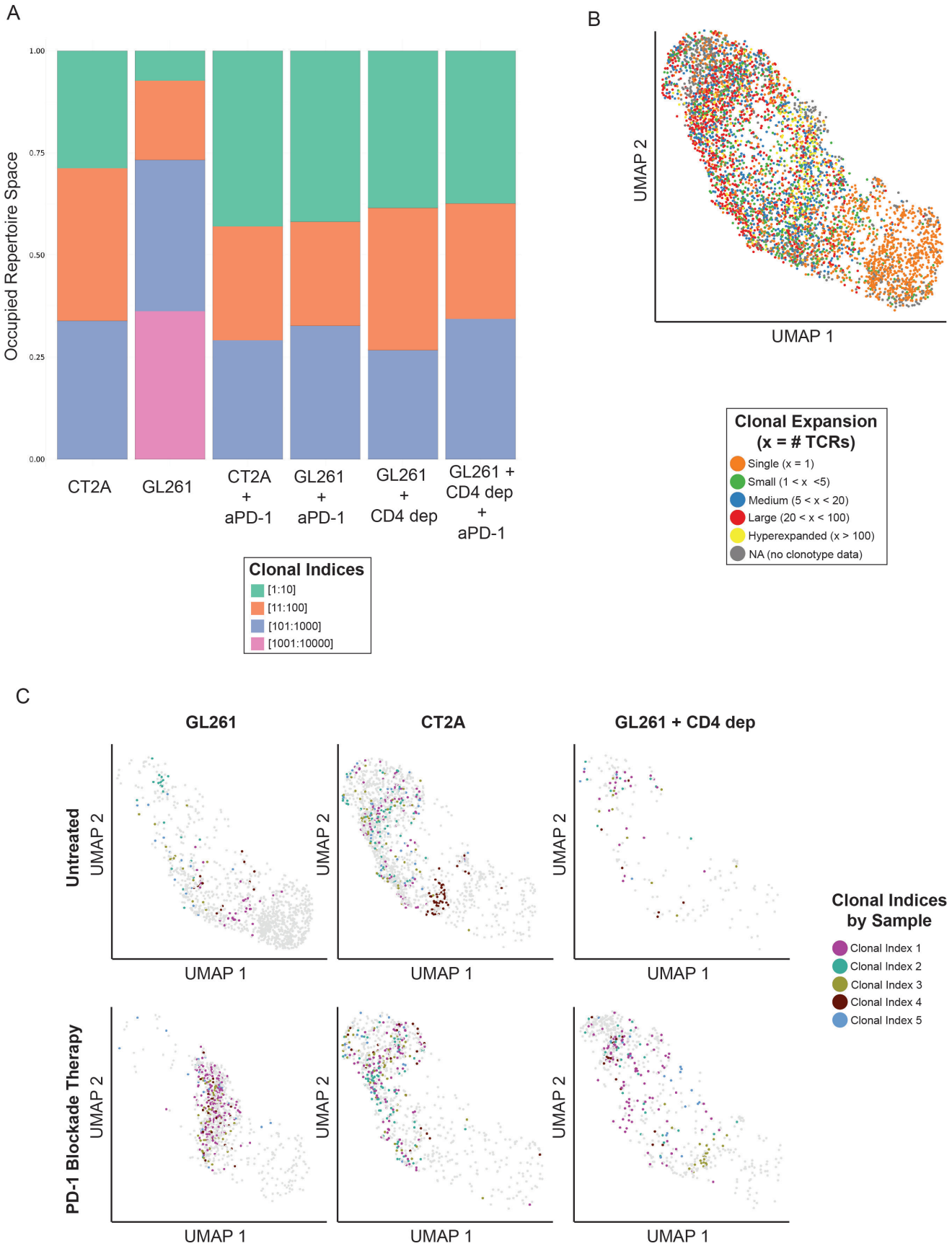

Figure 4 Tumor-infiltrating T-cell TCR clonality and diversity (A) TCR heterogeneity of each glioma model, wherein 'clonal index' represents each clonotype's rank-based frequency. (B) Clonal expansion categories superimposed onto UMAP of all conditions concatenated. (C) Visualization of the top five expanded clonotypes of each tumor model superimposed onto individual UMAP.

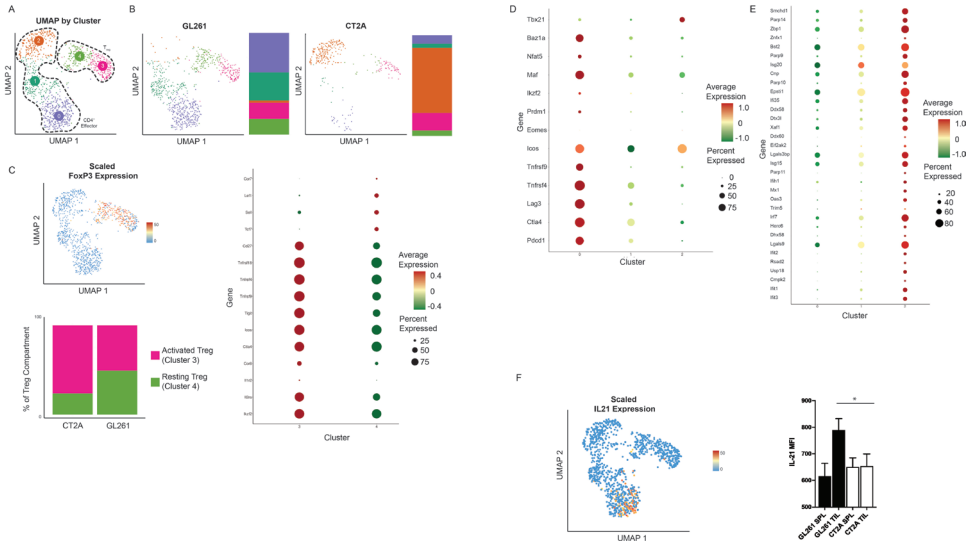

Figure 5 Single-cell RNA sequencing characterization of infiltrating CD4 T cells. (A) UMAP with cells colored according to graph-based cluster. (B) Graph-based clustering and cluster composition of the CD4 T-cell compartment separated by glioma model. (C) Characterization of the regulatory T-cell (T_{reg}) compartment: scaled *Foxp3* expression defines clusters 3 and 4 as T_{reg} (left/top); expression dot plot of key T_{reg} genes defines cluster 3 as activated and cluster 4 as resting T_{reg} (right); and histogram of T_{reg} composition shows CT2A is predominantly activated T_{reg}, while GL261 is composed of equivalent proportions of activated and resting T_{reg} (left/bottom). (D) Expression dot plot of effector CD4 T-cell genes in the non-T_{reg} clusters. (E) Expression dot plot of genes comprising the *Isc* signature, which is more highly expressed in cluster 2.[31] (F) Feature plot demonstrating scaled gene expression of *IL-21* (left) and bar graph depicting protein expression represented as mean fluorescent intensity of IL-21 within Foxp3$^-$ CD4$^+$ TIL (right; data pooled from at least two independent experiments with n=3 mice per group per experiment.; GL261 TIL vs CT2A TIL, p=0.030). IL, interleukin; TIL, tumor-infiltrating lymphocyte; T_{reg}, regulatory T cell.

reduction in clonal diversity (figure 4A,C). In contrast, we did not observe these effects in the T_{ex}^{term} predominant CT2A-depleted or CD4-depleted GL261 models (figure 4A,C). Specifically, the untreated GL261 CD8$^+$ TIL compartment was composed predominantly of minimally expanded TCRs, represented primarily by clonal indices of >100 (figure 4B). Conversely, the CD8 T-cell compartments of treated GL261, untreated and treated CD4-depleted GL261, and untreated and treated CT2A all exhibited significant clonal enrichment, with the top 100 clonal indices comprising more than 75% of the TCRs. Notably, each of these hyperexpanded clones appears to be distributed across multiple clusters (figure 4C), suggesting that T cells within a single clonal population exist at various stages of exhaustion. Taken together, while the T_{ex}^{prog}-enriched TILs of GL261 undergo a phenotypical and transcriptional transformation with a proliferative burst following PD-1 blockade therapy, no such changes are observed in the dysfunctional CD4 models and may underlie the differential responsiveness of each model to PD-1 blockade therapy.

CT2A is composed of inhibitory regulatory T cells and dysfunctional effector CD4 T cells relative to GL261

Given the effect of CD4 T cells on the T_{ex} population in each tumor model, we next analyzed the CD4 T-cell compartment from the untreated GL261 and CT2A TIL, consisting of 1103 cells and 14013 genes (figure 5). We analyzed the effect of tumor type on the CD4 T-cell compartment; while GL261 (figure 5B) was represented in clusters 0, 1, 3, and 4, the CD4 T-cell compartment of CT2A was primarily enriched in clusters 2 and 3 (figure 5B). We found two clusters (clusters 3 and 4) with high *Foxp3* expression indicative of regulatory T cells (T_{reg}) (figure 5C).[25] We next compared the expression of genes related to T_{reg} function to delineate resting versus activated states. *Tnfrsf9*, the costimulatory receptor for tumor necrosis factor family 4-1BB, is a marker of activated T_{reg}, which are capable of increased suppressive capacity of T-cell proliferation and activity.[26–28] We found *Tnfrsf9* to be highly expressed in the T_{reg} cluster 3, which is enriched in CT2A (figure 5C). Importantly, such activated T_{reg} populations are strongly correlated with poorer prognosis in both systemic and intracranial tumors, along with a lack of response to PD-1 blockade therapy in non-small cell lung cancer.[25]

We next compared the expression of a gene set associated with an exhausted CD4 T-cell state within the *Foxp3*-negative, effector CD4$^+$ clusters (clusters 0, 1, and 2).[29] Cluster 0, enriched in GL261, is marked by elevated expression of key markers of CD4 T-cell exhaustion such as *Pdcd1*, *Ctla4*, and *Lag3* (figure 5D). This was initially surprising as we anticipated CT2A, enriched in the T_{ex}^{term} subset, would similarly be composed of exhausted CD4 T cells. However, as previously demonstrated in bladder and head and neck cancers, exhausted CD4 T cells do not display the same dysfunction as their exhausted CD8 T-cell counterparts, and in specific contexts, CD4 T cells with an exhausted phenotype represent a checkpoint-responsive

subset with the potential to proliferate and increase cytokine production following therapy.[30] Gene ontology analysis of the top biological processes demonstrated the CT2A-enriched cluster 2 was associated with response to interferon-responsive genes (online supplemental figure S10), previously correlated with poor response to checkpoint therapy in the murine MC38 adenocarcinoma model.[31] Given this association, we quantified expression of a previously described gene signature defining a dysfunctional $CD4^+$ subset characterized by expression of type I interferon (IFN)-responsive genes (*Isc*) and associated with poor prognosis.[29 31] We found the *Isc* gene signature strongly associated with the CT2A effector CD4 T-cell cluster 2 compared with the GL261 effector CD4 T-cell clusters 0 and 1, further supporting a dysfunctional CT2A effector CD4 T-cell compartment (figure 5E). Finally, given the described role of IL-21 secretion by CD4 T cells in maintaining CD8 T cells in a non-terminal exhaustive state,[24 32] we next determined the subpopulations expressing this cytokine, noting restricted expression in the GL261-predominant cluster 0 (figure 5F). This increased expression of IL-21 in CD4 effector TIL from GL261 compared with CT2A was subsequently confirmed on a protein level by flow cytometry (figure 5F). *IL-21* was minimally expressed in the other CD4 effector clusters, suggesting a potential mechanism for the disparity of exhausted CD8 T-cell states in GL261 and CT2A.

Thus, scRNA-seq analysis reveals a balanced resting and activated T_{reg} ratio along with activated effector CD4 T cells in the PD-1 responsive GL261 model, which contrasts with the skewing toward an immunosuppressive, activated T_{reg}-enriched and *Isc*-expressing effector CD4 T-cell subsets in the CT2A model. Importantly, this analysis indicates that a functional CD4 T-cell compartment is key to maintaining PD-1 blockade responsiveness in glioblastoma models.

CD40 agonism synergizes with PD-1 blockade to provide protection in a CD4-dysfunctional but not a CD4-proficient brain tumor microenvironment

One mechanism by which effector CD4 T cells promote an effective CD8 T-cell antitumor immune response is via CD40–CD40 ligand (CD40L) interactions with dendritic cells to induce upregulation of MHC class I expression and co-stimulatory molecules, and secrete activating cytokines such as IL-12.[33 34] Therefore, CD40 agonists are actively being explored as both monotherapy and combinatorial therapies to improve the effector T-cell response in patients with advanced malignancies. Similarly, we hypothesized that a selective deficiency in CD4 T-cell functionality could be bypassed with CD40 agonism. To evaluate this hypothesis, mice with established intracranial CT2A were treated with CD40 agonist with or without PD-1 blockade. No survival benefit was observed with either CD40 or anti-PDL1 monotherapy (figure 6A). However, a significant survival benefit was observed following combinatorial therapy (figure 6), suggesting synergy between these two therapeutic targets. In stark contrast, the addition of CD40 agonist, either as monotherapy or in combination with PD-1 blockade, did not significantly improve survival in GL261-bearing mice (figure 6B). Of note, we delayed the initiation of PD-1 blockade to a later time point resulting in a lower survival rate (figure 6B) similar to what was seen in CT2A. This would allow detection of potential synergy as earlier administration of PD-1 blockade in GL261 has a high cure rate as a monotherapy (online supplemental figure S6). These results support prior findings that the addition of CD40 agonism may augment responsiveness to PD-1 blockade in settings where CD4 T-cell activity is deficient or dysfunctional but not in the context of a proficient effector CD4 T-cell response.

DISCUSSION

Standard of care therapy for primary glioblastoma entails gross total resection followed by concurrent temozolomide and radiation therapy; despite this aggressive regimen,

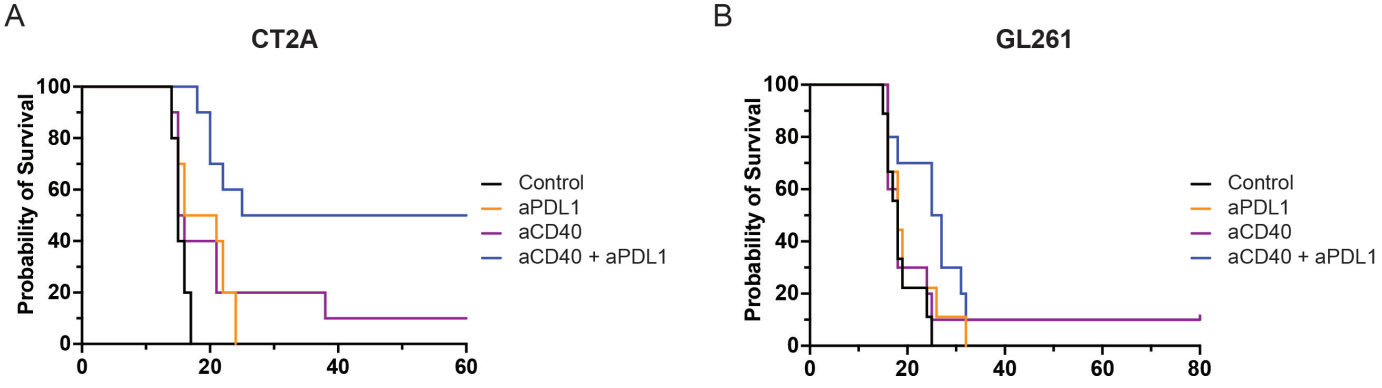

Figure 6 Circumventing a dysfunctional CD4 T-cell response through CD40 agonism. Kaplan-Meier survival curves evaluating CD40 agonist and PD-1 blockade monotherapy and combinatorial therapy in (A) CT2A (p=0.0003) and (B) GL261 (p=0.1129) demonstrate CD40 agonism delivers a synergistic benefit with PD-1-blockade therapy, exclusively in a CD4-deficient environment. For each experiment, n=5 per group and pooled from two independent experiments.

median survival from diagnosis remains less than 2 years.[1] Checkpoint blockade therapeutics have achieved durable responses across multiple malignancies. Unfortunately, despite the success of PD-1 blockade therapy to date, this therapeutic modality has yet to demonstrate efficacy in glioblastoma.

A fundamental understanding of treatment failure with checkpoint blockade therapy in patients with glioblastoma could identify strategies to overcome PD-1-blockade resistance and provide additional therapeutic options in an otherwise dismal pathology. One proposed mechanism of glioblastoma resistance to checkpoint blockade is T-cell dysfunction, first described in chronic LCMV infection and more recently demonstrated in murine glioma models.[14] For that reason, we leveraged scRNA-seq to explore complementary models of mouse glioblastoma with differing responsiveness to PD-1 blockade therapy, permitting investigation of mechanisms driving therapeutic resistance in brain tumors. We demonstrate presence of a predominant T_{ex}^{term} population associated with CD4-deficient, PD-1 blockade-resistant models (CT2A and CD4-depleted GL261), whereas a predominant T_{ex}^{prog} subset is associated with the CD4-proficient, PD-1 blockade-sensitive model (GL261). Importantly, we demonstrate a strategy using CD40 agonism to circumvent a dysfunctional CD4 T-cell response to induce PD-1 blockade responsiveness and provide a survival benefit in an otherwise unresponsive mouse glioblastoma model. Our findings complement prior descriptions of the GL261 and CT2A immunological microenvironment but importantly represent the first application of scRNA-seq to provide a higher-resolution comparative analysis of the CD4 and CD8 T-cell states and clonotypes in these models.[14 35]

While others have reported a dichotomous split of the CD8 T_{ex}^{prog} and T_{ex}^{term} states in models of chronic viral infection, more recently nuanced phenotypical diversity in the CD8 T-cell compartment has been reported by surface markers demonstrating transitional transcriptional states.[7 12 23 25] Additionally, shared clonotypes between the CD8 T-cell clusters have previously been demonstrated in systemic tumors and suggest a developmental pathway of exhaustion, further supported by scRNA-seq analyses, suggesting a progressive population between functional and dysfunctional CD8 T cells.[25] In fact, this predysfunctional compartment, defined by *Tcf7* expression, has been shown to be an integral population for the generation of an antitumor response to checkpoint inhibition in both mouse and human melanoma.[9–12] The treatment disparity between GL261 and CT2A is also consistent with the markedly reduced functionality of $CD8^+$ TIL observed in CT2A compared with other orthotopic brain tumor models.[14 35] Thus, we extend findings of a graded state of T-cell exhaustion well-defined in extracranial tumors to the GL261 and CT2A glioblastoma models.

Although CD4 T cells are required for response to PD-1 blockade therapy in cancer, the exact mechanism by which CD4 T cells mediate this effect remains unclear.[36] Direct CD4 T cell-mediated cytotoxicity has been reported following checkpoint blockade therapy in bladder cancer; however, a CD4-dependent survival benefit observed in MHC class II-negative tumors, like glioblastoma, suggests an additional indirect contribution by CD4 T cells.[37 38] Similarly, as GL261 does not express MHCII, the role of CD4 T cells in checkpoint blockade therapy is likely not through direct cytotoxicity. Thus, we present data that support a model whereby CD4 T cells facilitate PD-1 blockade responsiveness by maintaining CD8 T cells in a T_{ex}^{prog} transcriptional state poised for antitumor effect.

How CD4 T cells restrict CD8 T cells from developing into PD-1 blockade unresponsive T_{ex}^{term} also remains undefined. It is possible that effector CD4 T cells alter the tumor microenvironment to maintain the T_{ex}^{prog} population. For example, chronic LCMV viral infection models have demonstrated that CD4 T cells can revert an immunosuppressive environment generated by prolonged interferon signaling.[39] Additionally, murine melanoma models have demonstrated that anti-PD-1 therapy in the absence of CD4 T cells is unable to maintain a potent effector CD8 T-cell population.[24] Zander *et al* demonstrated in the B16 melanoma model that CD8 T cells with uniformly high PD-1 expression and an exhausted phenotype can recover function and significantly reduce tumor burden in an IL-21-dependent fashion following adoptive cell therapy of IL-21-producing CD4 T cells. Similarly, Ren *et al* demonstrated that a dysfunctional CD8 T-cell response due to CD4 depletion during a polyomavirus infection of the CNS may be recovered with intrathecal IL-21 delivery.[32] This is consistent with our scRNA-seq data, in which $CD4^+$ clusters from checkpoint-responsive GL261 express *IL-21*, whereas checkpoint-resistant CT2A $CD4^+$ clusters do not.

Another potential role of CD4 T cells in mounting an antitumor response is by activating intermediary immune subsets. Although MHCII-negative tumor cells may not be directly lysed by CD4 T cells, other MHCII-expressing subtypes (eg, dendritic cells, monocytes, macrophages, and microglia) within the brain tumor microenvironment may have a role in initiating an immune response through the secretion of stimulatory cytokines such as IFN-γ to recruit natural killer cells, eosinophils, and macrophages.[40] The relative contribution of each of these subsets to antitumor immunity requires further evaluation.

Given prior findings that CD4 deficiency can be circumvented to treat polyomavirus CNS infection, we selected CD40 agonists to offset a deficient CD4 T-cell compartment in CT2A.[32 41] CD40L is primarily expressed by activated CD4 T cells.[42] CD40 agonists act on dendritic cells to promote upregulation of MHC expression, CD86 costimulatory expression, expression of secondary costimulatory molecules (CD137 and OX40), and secretion of IL-12 to initiate an immunological reaction in a CD4-independent fashion.[33 34] Here, we corroborate a synergistic response with anti-PDL1 therapy in the context of a dysfunctional CD4 T-cell response in CT2A. Interestingly,

CD40 agonism provides no survival benefit with the functional CD4 T-cell compartment of GL261. Together, these data suggest CD40 agonism may have an immune stimulatory role in tumors deficient in CD4 T cells, such as glioblastoma.

Glioblastoma has been well established as a tumor defined by dysfunctional tumor-infiltrating T cells.[35] For example, in a recently published pan-cancer analysis of The Cancer Genome Atlas using gene set enrichment analyses from scRNA-seq to define the various T_{ex} subsets, glioblastoma was among the most enriched for the T_{ex}^{term} subgroup across all cancer histologies.[43] However, a comprehensive proteogenomic analysis of the glioblastoma-infiltrating T-cell compartment on a single-cell level is needed to fully characterize the degree of T-cell dysfunction in patients with glioblastoma and is the focus of ongoing work. Moreover, this dysfunctional T-cell compartment in glioblastoma is not limited to the TIL, as systemic lymphopenia, particularly CD4 lymphopenia, is observed secondary to T-cell sequestration in the bone marrow.[16] Such CD4 lymphopenia is exacerbated following temozolomide chemotherapy and radiation, often reaching levels observed in AIDS.[44 45] Given the observed role of CD4 T cells in maintaining the PD-1 blockade responsive T_{ex}^{prog} subset and preventing development of T_{ex}^{term} in these preclinical brain tumor models, it is reasonable to hypothesize that the enrichment of T_{ex}^{term} TIL and lack of PD-1 blockade efficacy in glioblastoma are due to CD4 T-cell depletion or dysfunction. Importantly, from a translational perspective, the observations from this study support the use of alternative strategies to overcome CD4 T-cell dysfunction, such as CD40 agonism, to provide synergistic improvement to PD-1 blockade therapy and warrant further testing in clinical trials.

Twitter Rupen Desai @RupenDesaiMD

Acknowledgements We thank the McDonnell Genome Institute for assistance with generating the single-cell RNA sequencing cDNA libraries.

Contributors GPD and TMJ conceived the project and designed experiments. AC and AL performed experiments. SMK and RD analyzed the data under supervision from AP and TMJ. RD wrote the manuscript with assistance from all authors. All authors reviewed the manuscript. TMJ served as guarantor.

Funding TMJ received a Paul Calabresi K12 Career Development Award for Clinical Oncology.

Competing interests None declared.

Patient consent for publication Not applicable.

Ethics approval This study involves mouse experimentation and was approved by the Washington University in St. Louis (Institutional Animal Care and Use Committee, protocol 19-0850).

Provenance and peer review Not commissioned; externally peer reviewed.

Data availability statement Data are available in a public, open access repository. Data are available upon reasonable request. Data are available in a public, open access repository. Data have been deposited on Zenodo and will become publicly available upon publication or request (DOI: 10.5281/zenodo.6522745).

ORCID iDs
Rupen Desai http://orcid.org/0000-0002-2052-7243
Gavin P Dunn http://orcid.org/0000-0001-9302-4834

REFERENCES

1 Desai R, Suryadevara CM, Batich KA, *et al*. Emerging immunotherapies for glioblastoma. *Expert Opin Emerg Drugs* 2016;21:133–45.
2 Wolburg H, Noell S, Fallier-Becker P, *et al*. The disturbed blood-brain barrier in human glioblastoma. *Mol Aspects Med* 2012;33:579–89.
3 Tawbi HA, Forsyth PA, Algazi A, *et al*. Combined nivolumab and ipilimumab in melanoma metastatic to the brain. *N Engl J Med Overseas Ed* 2018;379:722–30.
4 Blackburn SD, Shin H, Freeman GJ, *et al*. Selective expansion of a subset of exhausted CD8 T cells by alphaPD-L1 blockade. *Proc Natl Acad Sci U S A* 2008;105:15016–21.
5 Wherry EJ, Ha S-J, Kaech SM, *et al*. Molecular signature of CD8+ T cell exhaustion during chronic viral infection. *Immunity* 2007;27:670–84.
6 Im SJ, Hashimoto M, Gerner MY, *et al*. Defining CD8+ T cells that provide the proliferative burst after PD-1 therapy. *Nature* 2016;537:417–21.
7 Utzschneider DT, Charmoy M, Chennupati V, *et al*. T Cell Factor 1-Expressing Memory-like CD8(+) T Cells Sustain the Immune Response to Chronic Viral Infections. *Immunity* 2016;45:415–27.
8 Beltra J-C, Manne S, Abdel-Hakeem MS, *et al*. Developmental Relationships of Four Exhausted $CD8^+$ T Cell Subsets Reveals Underlying Transcriptional and Epigenetic Landscape Control Mechanisms. *Immunity* 2020;52:825–41.
9 Kurtulus S, Madi A, Escobar G, *et al*. Checkpoint Blockade Immunotherapy Induces Dynamic Changes in $PD^-1^-CD8^+$ $Tumor^-$ Infiltrating T Cells. *Immunity* 2019;50:181–94.
10 Miller BC, Sen DR, Al Abosy R, *et al*. Subsets of exhausted $CD8^+$ T cells differentially mediate tumor control and respond to checkpoint blockade. *Nat Immunol* 2019;20:326–36.
11 Sade-Feldman M, Yizhak K, Bjorgaard SL, *et al*. Defining T cell states associated with response to checkpoint immunotherapy in melanoma. *Cell* 2018;175:998–1013.
12 Siddiqui I, Schaeuble K, Chennupati V, *et al*. Intratumoral $Tcf1^+PD$-1^+CD8^+ T Cells with Stem-like Properties Promote Tumor Control in Response to Vaccination and Checkpoint Blockade Immunotherapy. *Immunity* 2019;50:195–211.
13 Johanns TM, Ward JP, Miller CA, *et al*. Endogenous Neoantigen-Specific CD8 T cells identified in two glioblastoma models using a cancer Immunogenomics approach. *Cancer Immunol Res* 2016;4:1007–15.
14 Liu CJ, Schaettler M, Blaha DT, *et al*. Treatment of an aggressive orthotopic murine glioblastoma model with combination checkpoint blockade and a multivalent neoantigen vaccine. *Neuro Oncol* 2020;22:1276–88.
15 Day CL, Kaufmann DE, Kiepiela P, *et al*. Pd-1 expression on HIV-specific T cells is associated with T-cell exhaustion and disease progression. *Nature* 2006;443:350–4.
16 Chongsathidkiet P, Jackson C, Koyama S, *et al*. Sequestration of T cells in bone marrow in the setting of glioblastoma and other intracranial tumors. *Nat Med* 2018;24:1459–68.
17 Aslan K, Turco V, Blobner J, *et al*. Heterogeneity of response to immune checkpoint blockade in hypermutated experimental gliomas. *Nat Commun* 2020;11:931.
18 Stuart T, Butler A, Hoffman P, *et al*. Comprehensive integration of single-cell data. *Cell* 2019;177:1888–902.
19 Aran D, Looney AP, Liu L, *et al*. Reference-Based analysis of lung single-cell sequencing reveals a transitional profibrotic macrophage. *Nat Immunol* 2019;20:163–72.

20 Petti AA, Williams SR, Miller CA, *et al*. A general approach for detecting expressed mutations in AML cells using single cell RNA-sequencing. *Nat Commun* 2019;10:3660.
21 Wu T, Hu E, Xu S, *et al*. clusterProfiler 4.0: a universal enrichment tool for interpreting omics data. *Innovation* 2021;2:100141.
22 Borcherding N, Bormann NL, Kraus G. scRepertoire: an R-based toolkit for single-cell immune receptor analysis. *F1000Res* 2020;9:47.
23 Fehlings M, Simoni Y, Penny HL, *et al*. Checkpoint blockade immunotherapy reshapes the high-dimensional phenotypic heterogeneity of murine intratumoural neoantigen-specific $CD8^+$ T cells. *Nat Commun* 2017;8:562.
24 Zander R, Schauder D, Xin G, *et al*. $CD4^+$ T Cell Help Is Required for the Formation of a Cytolytic $CD8^+$ T Cell Subset that Protects against Chronic Infection and Cancer. *Immunity* 2019;51:1028–42.
25 Guo X, Zhang Y, Zheng L, *et al*. Global characterization of T cells in non-small-cell lung cancer by single-cell sequencing. *Nat Med* 2018;24:978–85.
26 Lubrano di Ricco M, Ronin E, Collares D, *et al*. Tumor necrosis factor receptor family costimulation increases regulatory T-cell activation and function via NF-κB. *Eur J Immunol* 2020;50:972–85.
27 Zhang P, Gao F, Wang Q, *et al*. Agonistic anti-4-1BB antibody promotes the expansion of natural regulatory T cells while maintaining FOXP3 expression. *Scand J Immunol* 2007;66:435–40.
28 Elpek KG, Yolcu ES, Franke DDH, *et al*. Ex vivo expansion of CD4+CD25+FoxP3+ T regulatory cells based on synergy between IL-2 and 4-1BB signaling. *J Immunol* 2007;179:7295–304.
29 Crawford A, Angelosanto JM, Kao C, *et al*. Molecular and transcriptional basis of $CD4^+$ T cell dysfunction during chronic infection. *Immunity* 2014;40:289–302.
30 Balança C-C, Salvioni A, Scarlata C-M, *et al*. Pd-1 blockade restores helper activity of tumor-infiltrating, exhausted PD-1hiCD39+ CD4 T cells. *JCI Insight* 2021;6:e142513.
31 Magen A, Nie J, Ciucci T, *et al*. Single-Cell Profiling Defines Transcriptomic Signatures Specific to Tumor-Reactive versus Virus-Responsive $CD4^+$ T Cells. *Cell Rep* 2019;29:3019–32.
32 Ren HM, Kolawole EM, Ren M, *et al*. Il-21 from high-affinity CD4 T cells drives differentiation of brain-resident CD8 T cells during persistent viral infection. *Sci Immunol* 2020;5:eabb5590.
33 Ridge JP, Di Rosa F, Matzinger P. A conditioned dendritic cell can be a temporal bridge between a CD4+ T-helper and a T-killer cell. *Nature* 1998;393:474–8.
34 Sotomayor EM, Borrello I, Tubb E, *et al*. Conversion of tumor-specific CD4+ T-cell tolerance to T-cell priming through in vivo ligation of CD40. *Nat Med* 1999;5:780–7.
35 Woroniecka K, Chongsathidkiet P, Rhodin K, *et al*. T-Cell exhaustion signatures vary with tumor type and are severe in glioblastoma. *Clin Cancer Res* 2018;24:4175–86.
36 Homet Moreno B, Zaretsky JM, Garcia-Diaz A, *et al*. Response to programmed cell death-1 blockade in a murine melanoma syngeneic model requires costimulation, CD4, and CD8 T cells. *Cancer Immunol Res* 2016;4:845–57.
37 Gubin MM, Zhang X, Schuster H, *et al*. Checkpoint blockade cancer immunotherapy targets tumour-specific mutant antigens. *Nature* 2014;515:577–81.
38 Oh DY, Kwek SS, Raju SS, *et al*. Intratumoral $CD4^+$ T Cells Mediate Anti-tumor Cytotoxicity in Human Bladder Cancer. *Cell* 2020;181:1612–25.
39 Wilson EB, Yamada DH, Elsaesser H, *et al*. Blockade of chronic type I interferon signaling to control persistent LCMV infection. *Science* 2013;340:202–7.
40 Charles NA, Holland EC, Gilbertson R, *et al*. The brain tumor microenvironment. *Glia* 2011;59:1169–80.
41 Vonderheide RH, Flaherty KT, Khalil M, *et al*. Clinical activity and immune modulation in cancer patients treated with CP-870,893, a novel CD40 agonist monoclonal antibody. *J Clin Oncol* 2007;25:876–83.
42 Vonderheide RH. Cd40 agonist antibodies in cancer immunotherapy. *Annu Rev Med* 2020;71:47–58.
43 Zhang Z, Chen L, Chen H, *et al*. Pan-Cancer landscape of T-cell exhaustion heterogeneity within the tumor microenvironment revealed a progressive roadmap of hierarchical dysfunction associated with prognosis and therapeutic efficacy. *EBioMedicine* 2022;83:104207.
44 Grossman SA, Ellsworth S, Campian J, *et al*. Survival in patients with severe lymphopenia following treatment with radiation and chemotherapy for newly diagnosed solid tumors. *J Natl Compr Canc Netw* 2015;13:1225–31.
45 Campian JL, Piotrowski AF, Ye X, *et al*. Serial changes in lymphocyte subsets in patients with newly diagnosed high grade astrocytomas treated with standard radiation and temozolomide. *J Neurooncol* 2017;135:343–51.